Building Simulation 2009

Eleventh International IBPSA Conference
Glasgow, Scotland
July 27-30, 2009

TOTAL UTILITY DEMAND PREDICTION BASED ON PROBABILISTICALLY GENERATED BEHAVIROAL SCHEDULES OF ACTURAL INHABITANTS

Jun Tanimoto and Aya Hagishima
Interdisciplinary Graduate School of Engineering Sciences, Kyushu University

ABSTRACT
This paper describes a new methodology in calculating accurately the time series utility loads (energy, power, city water, hot water, etc.) in a dwelling. This calculation takes into account the behavioral variations of the dwelling inhabitants. The proposed method contains a procedure for cooling load calculations based on a series of Monte Carlo simulations where the HVAC on/off state and the indoor heat generation schedules are varied, time-step by time-step. A data set of time-varying inhabitant behavior schedules, with a 15 minute resolution, generated by the authors in previous studies and validated by a comparison analysis to several field measurement data sets, was integrated into the model. The established model, which is called the Total Utility Demand Prediction System (TUD-PS) can be applied to, for example, accurate estimation of an integrated space maximum requirement, such as the total load of a building or an urban area. In a series of numerical experiments, huge discrepancies were found between the conventional results and those considering the time-varying inhabitant behavior schedules. In particular, deriving the dynamic state change, of having the HVAC on/off from the inhabitant's schedules, was found to be a significant factor in the maximum cooling and heating loads.

KEYWORDS
Total utility demand prediction, High time-resolution, Probabilistic inhabitants behavior schedule, Probabilistic HVAC turning On/Off events, Residential building

1. INTRODUCTION

The Co-Generation System (CGS) has been regarded as one of the most effective methods in achieving high efficiency in terms of building energy conservation, leading to reduce CO_2 emissions. Recent development of compact CGSs, such as fuel cells, encourages rapid dissemination in the residential building market, in systems which we call Home Co-Generation Systems (H-CGS). It is well known that a high time-resolution prediction is required for both power and thermal demands to derive the most efficient operation, and the most effective designs because CGS provides power and hot water simultaneously. In general, a residential space has a greater hot water demand compared to an office space. But actual demand varies substantially among different dwellings because hot water demand is affected by the daily schedules of its inhabitants, showing typical stochastic features. Hence, multiplying the predictions simply for a set of dwellings, such as a residential building, a residential block, or even a city area, assuming a "standard dwelling" and a "standard schedule" seems inappropriate. Such a procedure leads to unrealistic and over estimated peak values. Therefore, we have been developing a novel framework for predicting high-time resolution utility demands in a dwelling or aggregated dwellings, considering various stochastic processes such as the schedules of the inhabitants, meteorology, etc. Firstly, we developed a stochastic model to deal with the probabilistic events for turning the HVAC on/off, based on the Markov Chain Theory (Tanimoto et al., 2005). We also presented a time-varying raw data of the schedules of the inhabitants (15 minute resolution), and a generating algorithm that utilizes only a statistical database available publicly (Tanimoto et al., 2008 a, b, and c). The algorithm is based on the "generate & kill" process. This method of generating the behavioral schedule for each individual does not produce a utility demand time series directly; however, by defining the links between each behavior and an energy-consuming event (plus its unit demand), we can convert that into a respective time series for electricity, gas, water, hot-water, etc. This method can provide a time series for indoor anthropogenic heat generation in respective rooms of a dwelling, but fall short of obtaining the cooling and heating load because it requires a dynamic thermal load calculation that considers the thermal characteristics of the building and every aspect of the stochastic processes. We developed the Total Utility Demand Prediction System (TUD-PS), where the building thermal system model and the stochastic inhabitant behavior schedule model are considered simultaneously in the form of a dynamic numerical prediction system, predicting the thermal load, power, gas, water, hot water demand, etc., with a 15 minute time resolution. Using TUD-PS, one can predict the utility demands of any residential building or area accurately, superposing the respective dwellings through Monte-Carlo simulation with a high time resolution. In particular, this paper discusses the structure of TUD-PS, the results of studies of the annual aggregate, and maximum thermal loads of a single dwelling. The proposed solution constitutes an alternative to previous methods for thermal load calculation assuming constant daily and deterministic HVAC

operation, and indoor anthropogenic heat generation, although those assumptions are known to have a crucial influence on the predicted results.

2. TUD-PS

The TUD-PS can reproduce the thermal load, power demands for lighting, other electric household appliances, domestic hot water, and the city water demands considering the actual variations in the behavioral schedules of the inhabitants, which differs daily among the dwellings. The time resolution is 15 minutes. The overall structure of TUD-PS is schematically shown in Fig. 1

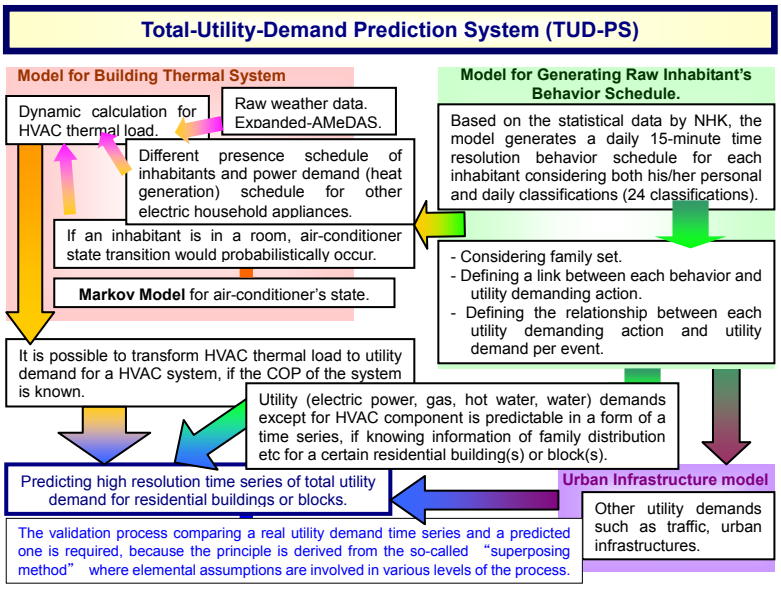

Figure 1. Holistic structure of TUD-PS.

The detail of the methodology, except for the thermal load calculation is referenced in our previous work (Tanimoto et al., 2008 a, b, and c). The framework for the dynamic analysis of building thermal systems is also derived from our previous model (Tanimoto & Kimura, 1990). Some fundamental equations are supplemented in the Appendix. Other assumptions are summarized in Table 1. The calculation main routine after the time discrete process is shown in Fig. 2. The data for the behavioral schedule of the inhabitants, prepared in advance as a data set of 10^5 samples having 24 classes (eight classes for inhabitant attributes, such as working male, housewife, etc, and three classes for weekdays, Saturdays and holidays), is incorporated for each dwelling at the beginning of each day after importing the climate data for the entire period (15 years, for the present cases) aggregately. At the commencement of the dwelling routine, standby power consumption is calculated based on a list of electric household appliances and the performance data for each dwelling. The imported behavioral schedule data determines the number of family members present and their activity in each room at any given time (the time resolution is 96 pixels in a day because 24 hours = 96 * 15 minutes), which defines the time series for electric power and gas demand, except for the daily demands for HVAC, hot water, and city water.

Concerning HVAC thermal load calculation, two layers of stochastic processes are considered. The first layer determines the heating and the cooling periods. We made particular correlation functions between the daily heating and cooling occurrences and the daily minimum and maximum outdoor air temperature for 10 day periods from 2001 to 2003, in a Sigmoid-shape function based on Mizutani's field measurement data (2006) acquired from hundreds of actual dwellings. This determines probabilistically whether a certain day is under a heating, cooling, or non air-conditioning period, but never indicates an actual thermal load. The second process is turning the HVAC on/off. This event is defined probabilistically after every 15 minutes by state transition functions $P(T)$, as shown in Table 2, where T is either the indoor globe temperature or outdoor air temperature in case of an off -> on or on -> on event (i.e., the complementary event of on -> off). The second process determines whether an actual thermal load occurs in the room.

Table 1 Assumptions for the thermal system model.

- Time backward (implicit) Finite Difference Method (r = 1, Δt = 15minites; cf. Eq.(8)).
- Air temperatures for non-air-conditioned rooms, crawl spaces under floor and rooms of the neighboring dwelling are given by $r_{out}T_{out} + (1 - r_{out})T_r$, where r_{out} is 0.5, 0.5, and 0.25, respectively.
- Equivalent heat capacity of indoor furniture per unit room air volume is assumed as 1/5 of that for office spaces (cf. Eq.(5)).
- Openings;
  When HVAC is on, a window is always closed (n_r = 0.2 h^{-1}). In heating period (winter), a curtain is opened if global horizontal solar radiation rate (GHSR) > 116 Wm^{-2}. In cooling period (summer), a curtain is closed if GHSR > 116 Wm^{-2}, otherwise opened. In spring or fall, a curtain is always opened.
  When the HVAC is off and in winter, a window is always closed and a curtain is opened if GHSR > 0 Wm^{-2}, otherwise closed. In spring and fall, a window is always closed and a curtain is always opened. In summer, a window is always opened (n_r = 1.0 h^{-1}) and a curtain is closed if GHSR > 116 Wm^{-2}, otherwise opened.
- Convective heat transfer coefficient; h_{c_in} = 4.7 and h_{c_out} = 23.3 $Wm^{-2}K^{-1}$ (cf.Eq.(3),(1))).
- Solar absorbance and emissivity for exterior walls are 0.75 and 0.85, respectively. Emissivity for indoor walls is 0.9.
- Set room air temperature for both heating and cooling are 20 °C and 26 °C, respectively. Set relative humidity is 50%. A calculated sensitive thermal load is obtained disregarding HVAC capacity. A latent thermal load is calculated by assuming a room vapor mass-balance equation disregarded vapor absorption/ desorption at indoor walls.

3. SETTING FOR NUMERICAL EXPERIMENT

The present study assumes both typical apartment dwellings and a typical detached house. The former

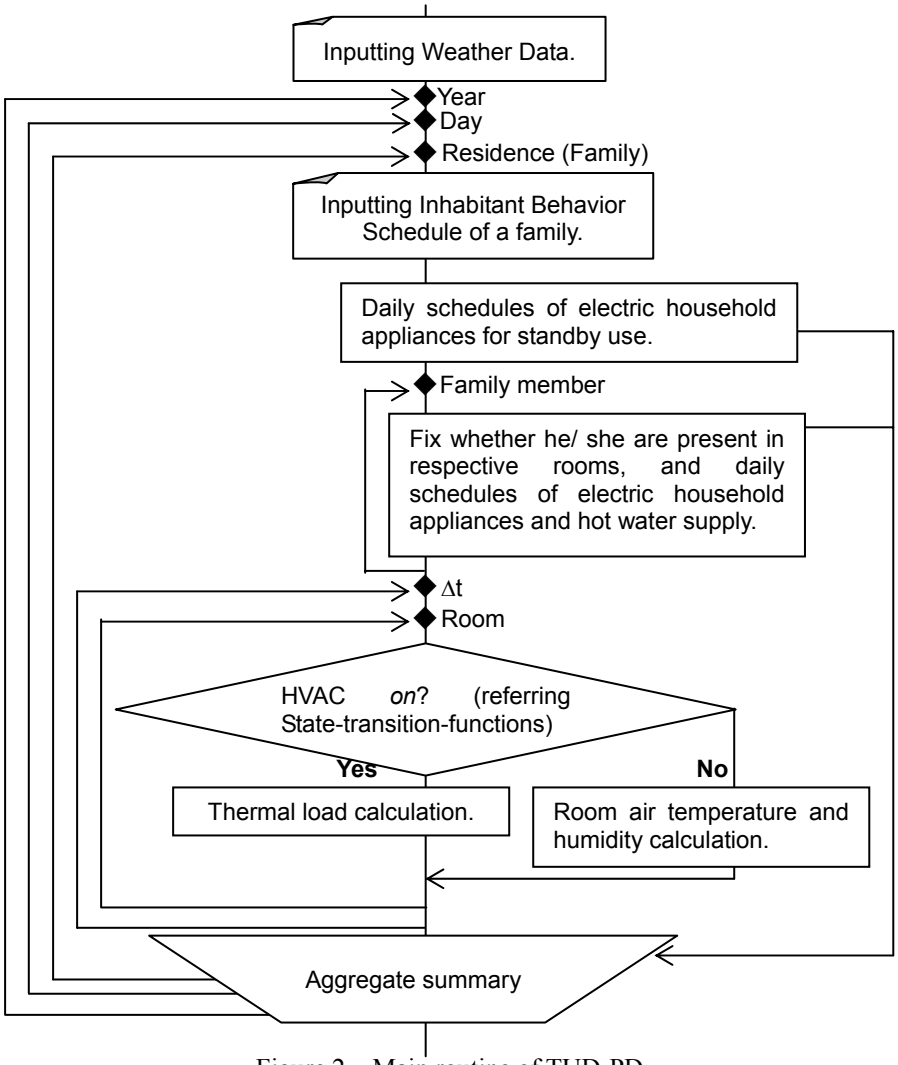

Figure 2 Main routine of TUD-PD.

Table 2 Assumed state transition functions.

	$P(T)$	
Cooling	**Off -> On** ***T*; indoor globe temperature** $a = 1.850, \theta = 32.2$	**On-> On** ***T*; Outdoor air temperature** $a = 1.285, \theta = 31.6$
Heating	**Off -> On** ***T*; indoor globe temperature** $a = 2.000, \theta = 18.5$	**On-> On** ***T*; Outdoor air temperature** $a = 2.000, \theta = 23.0$

- Function shape is *Sigmoid Function*; $P(T) = \frac{1}{1 + a^{-(T-\theta)}}$.
- Cooling case is derived from Tanimoto et al (2005). Parameters for heating case are purely assumed based on the cooling results.

class has nine sub types: East corner (total floor area is 101 m^2, consisting of a living and dining room, kitchen, one Japanese tatami room, and three bedrooms), center (total floor area 80.4 m^2, consisting of a living and dining room, kitchen, one Japanese tatami room, and two bedrooms) and west corner (total floor area 95.8 m^2, consisting of a living and dining room, kitchen, one Japanese tatami room, and three bedrooms). These three types are located on the top, middle, and first storey of the apartment, respectively. A standard plan for the thermal system analysis authorized by Architectural Institute of Japan (AIJ) is assumed to be a detached house (two storey, total floor area 125.9 m^2, consisting of a living and dining room, kitchen, one Japanese tatami room, and four bedrooms). All dwellings face south, and the insulation thickness of the exterior walls is assumed to be 50 mm. A family consisting of a father (working male), mother (housewife), two children (junior high school and elementary school pupils), live in each dwelling. The location is Tokyo, and the meteorological condition uses the unprocessed data from 1981 to 1995 of the Expanded AMeDAS (Akasaka et al, 2000).

We assumed four schedule settings. The default case is completely stochastic, where both indoor anthropogenic heat generation (from household appliances and inhabitants) and HVAC on/off schedules vary daily. We call this a stochastic schedule case. In contrast, deterministic heat generation assumes stochastic HVAC control, but deterministic anthropogenic heat generation, derived from the average of 10^5 vary in their schedules. Also, a deterministic HVAC schedule implies a stochastic anthropogenic heat generation but deterministic HVAC control, derived from the by and large assumed on/off schedule adopted in the previous simulation studies (SHASE Technical Report, 2000). In addition to these, there are two

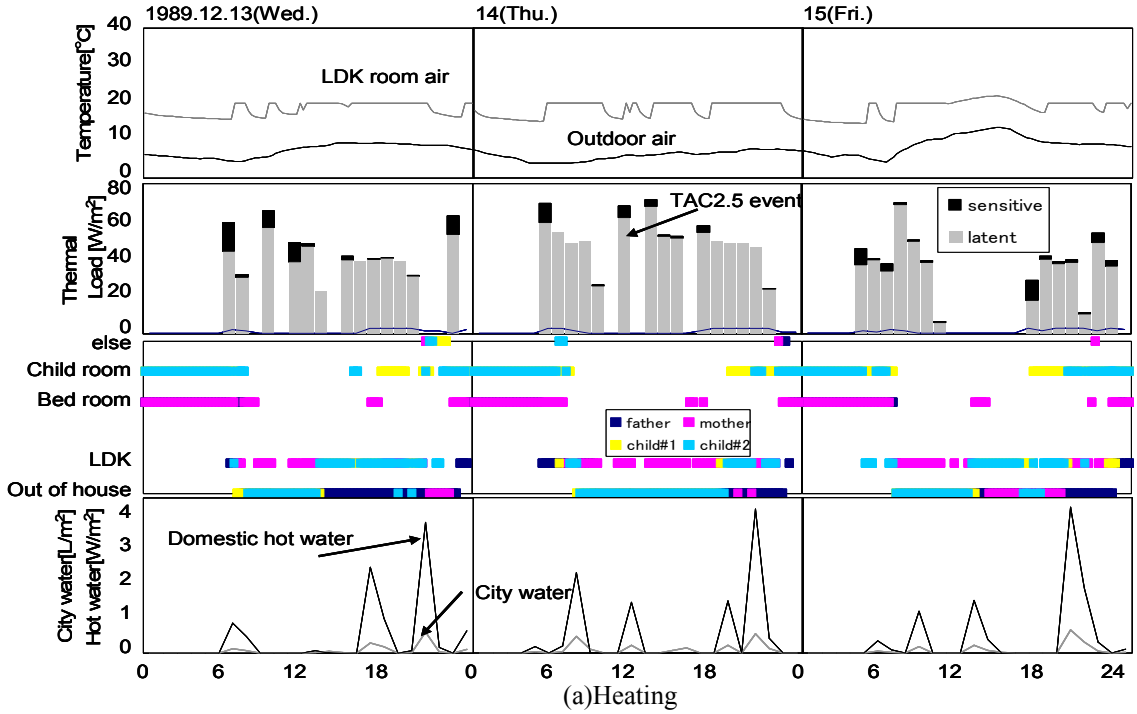

(a)Heating

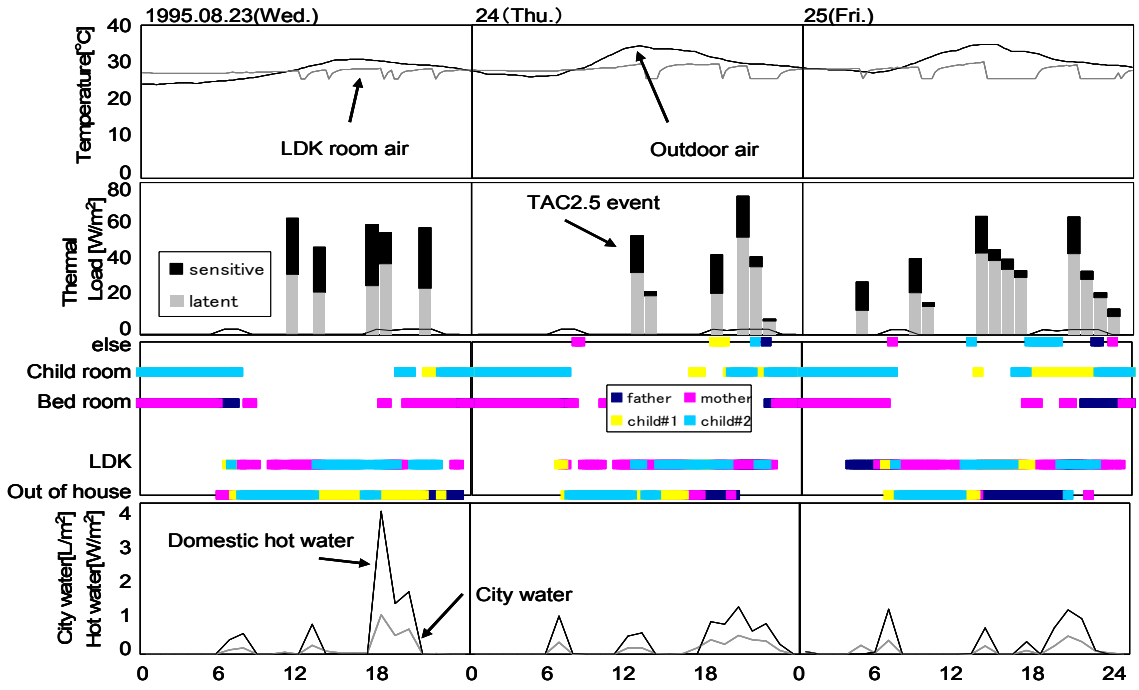

(b) Cooling

Figure 3 Time varying characteristics of the peak day for stochastic scheduling.

completely deterministic schedules. Both assume that anthropogenic heat generation and HVAC control schedules are deterministic. The first schedule particularly, which we call the completely deterministic schedule case #1, determines whether a day is in a heating, cooling or non air-conditioning period stochastically, through the procedure previously mentioned. In the second case, the completely deterministic schedule case #2, both cooling (from July to September) and heating (from December to March) periods are assumed deterministically.

4. RESULTS AND DISCUSSION

The standard case below reflects mainly that of a center and middle storey apartment.

4.1. Time varying characteristics of the peak day

Figure 3 shows result of the stochastic schedule when the maximum heating and cooling loads take place based on TAC 2.5% (overload risk 2.5%). The figure shows a day previous to and a following one to the peak load day in a time series. The varying

results of the indicated time are averaged over each hour, although TUD-PS predictions have a resolution of 15 minutes.

In the heating case, TAC 2.5% maximum (71.5 W/m^2 at 12:00 Dec. 14, 1989) takes place when the housewife returns to the living and dining room for her lunch, and turns on the HVAC. In the cooling case, the maximum (51.8 W/m^2 at 13:00 Aug. 24, 1995) takes place when the housewife turns the HVAC on due to overheating from a large solar heat gain.

4.2. Impact of stochastic schedules

4.2.1. Annual aggregate load

Figure 4 shows annual aggregated heating and cooling loads for all five cases that provides different schedule handling. Each bar indicates an averaged aggregate value over 15 years, and the numbers just above the bar indicates averaged aggregate heating and cooling hours.

The effect of using stochastic schedules, for HVAC especially, seems obvious. Comparing cooling loads between the stochastic schedule and the deterministic HVAC schedule shows that the discrepancy is significant.

It is noticeable that completely deterministic schedule case #2 is much larger than the stochastic schedule. The completely deterministic schedule case #2 uses almost same methodology that we have been assuming in practical or even research calculations so far. Hence, this comparison implies that the conventional calculation procedure contains huge errors vis-à-vis our proposed TUD-PS from the stochastic scheduling point of view.

4.2.2. TAC 2.5% maximum load

Figure 5 shows sorted one-hour average loads of the living-dining room, where bold gray, black, and solid black lines indicate the stochastic schedule, the completely deterministic schedule cases #1 and #2, respectively. Each vertical line shows an overload risk 2.5% point for all HVAC operating hours during 15 years. Note that there are significant discrepancies between the stochastic and deterministic cases. For cooling, the maximum load in the stochastic schedules is much larger than the deterministic prediction. Thus, considering a stochastic HVAC control schedule increases the maximum load, compared with the conventional, deterministic HVAC schedule (this result is not shown in Fig. 5 (b)).

4.3. Impact of inhabitant's tolerance to thermal conditions

We investigated the sensitivity of inhabitant's tolerance for thermal comfort on accumulated annual loads by changing parameter θ of the state transition functions shown in Table 2. For example, increasing the cooling $P(T)$ of off ->on by +1 $^\circ$C implies inhabitants having an energy conserving attitude, whereas a shift of −1 $^\circ$C means that the inhabitants are wasting energy.

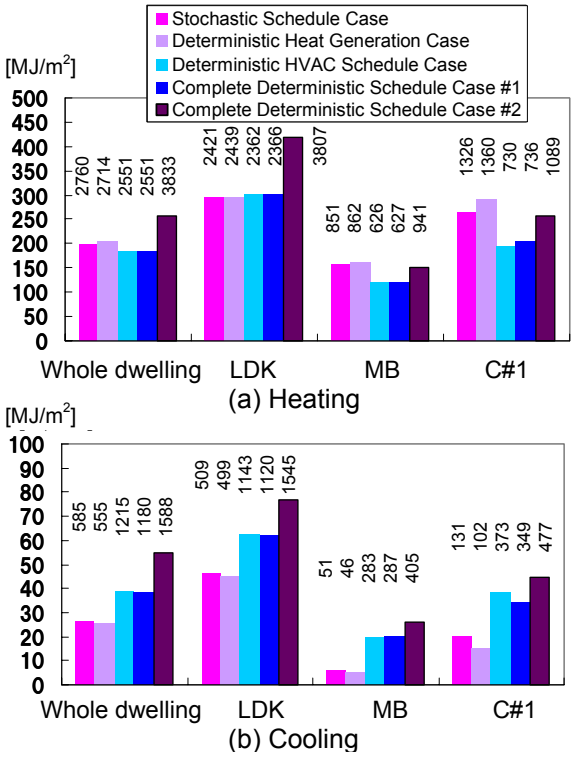

Figure 4 Averaged annual aggregate (a) heating and (b) cooling loads and their averaged annual operating hours over 15 years. LDK, MB and C#1 indicate the living-dining & kitchen, main bed room, and children's room, respectively.

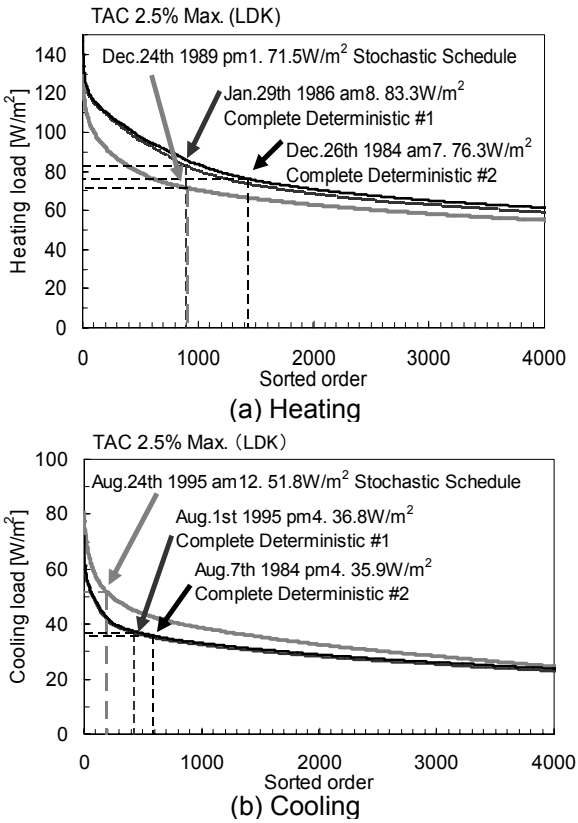

Figure 5 TAC 2.5% maximum (a) heating and (b) cooling loads over 15 years.

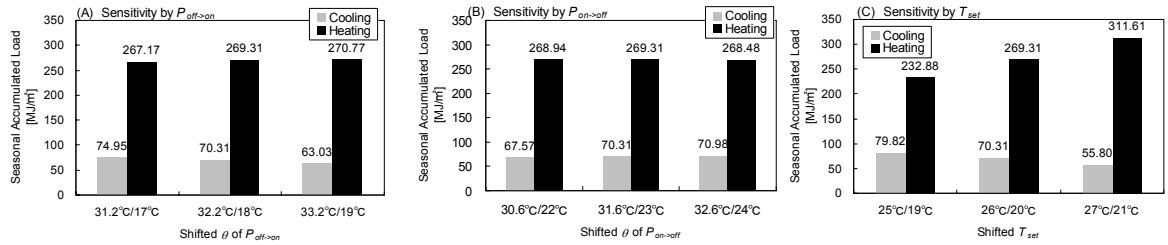

Figure 6 Sensitivity of aggregated annual loads by (a) off -> on $P(T)$, (b) on -> off $P(T)$ and (c) set air temperature.

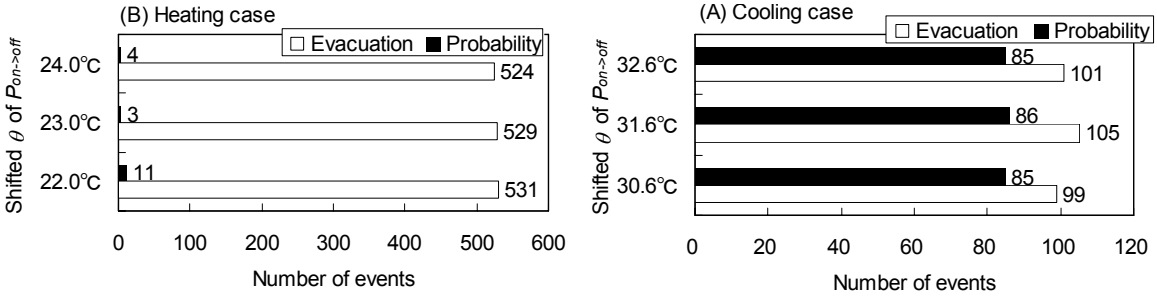

Figure 7 Event frequencies for leaving the room or inhabitants' behavior in turning off the HVAC.

In Fig. 6, (A) indicates sensitivity of θ (by adding ± 1 °C to the default values of 32.3 °C (cooling) and 18 °C (heating)) for off -> on $P(T)$ (e.g., HVAC turn-on sensitivity on the living-dinning room thermal load), while keeping on ->off $P(T)$ the default function; (B) indicates the sensitivity of θ for on -> off $P(T)$ (e.g., HVAC turn-off sensitivity on the thermal load) while keeping off ->on $P(T)$ the default function; and (C) shows sensitivity to the set air temperature (adding ± 1 to the default values of 26 °C (cooling) and 20 °C (heating)), while assuming the default state transition functions. Note that maintaining an enduring and additional temperature of 1 °C before turning on the HVAC can afford a 10.4% energy conservation effect for cooling and 0.8% for heating, although the maintenance of an enduring and additional temperature is less influential than shifting the set air temperature by ±1 °C.

Figure 7 shows whether inhabitant's leaving the room or their decision makes HVAC turning off in the simulation.

In cooling case, there are almost same frequencies (number of actual events) between those two situations. In heating case, HVAC is almost terminated by an event where the last inhabitant leaves the living-dining room. In the present simulation, HVAC is compulsorily turned off when no one is in the room. This is one reason for which we observe an irregular sensitivity to heating in Fig. 6 (B).

4.4. Different dwelling types

Tables 3 and 4 summarize the effect of stochastic schedules on aggregate and maximum loads for different dwelling types, either an apartment or a detached dwelling.

In all cases, there are significant discrepancies between the stochastic schedule we are proposing in the present paper and the four deterministic cases. Particularly, huge differences exist between the stochastic schedule and completely deterministic schedule case #2, which may imply that the conventional procedure entails disagreeable errors in its estimated aggregate and maximum loads.

5. CONCLUSION

In order to predict the utility demands accurately with a high time resolution for a residential sector, superposing respective dwellings through the Monte-Carlo simulation, we established a Total Utility Demand Prediction System (TUD-PS). Here both the building thermal system model and the inhabitant's stochastic behavioral schedule model are considered simultaneously in the form of a dynamic numerical prediction system, which enables 15 minute time resolution prediction of thermal load, power, gas, water, hot water demand, etc.

We have shown the importance of considering the stochastic schedules of both indoor anthropogenic heat generation and HVAC control due to inhabitant behavior, observing a series of simulation results of annual aggregate and maximum thermal loads for a single dwelling.

ACKNOWLEDGEMENT

This research was supported partially by a Grant-in-Aid for Scientific Research by JSPS, awarded to Dr. Hagishima (#20686040), and by the Kajima Research Foundation, the JUDANREN Foundation, and the Japan Securities Research Foundation. We would like to express gratitude to these funding sources. Prof. Inoue, Tokyo

Table 3 Summarized result of various dwelling types for heating.

Heating			Annual aggregated load [MJ/m^2]					TAC 2.5% maximum load [W/m^2]				
			Stochastic	Deterministic heat	Deterministic HVAC	Complete de-terministic #1	Complete de-terministic #2	Stochastic	Deterministic heat	Deterministic HVAC	Complete de-terministic #1	Complete de-terministic #2
East Corner	Top	Whole	187.6	236.3	180.1	219.1	282.8	58.7	64.4	52.8	57.8	57.8
		LDK	232.7	349.6	256.5	357.0	474.2	101.0	119.2	132.5	144.4	133.8
	Middle	Whole	156.5	214.9	148.7	198.2	263.1	39.5	45.1	39.1	44.3	41.9
		LDK	162.2	303.0	167.6	293.6	405.4	55.4	72.9	68.6	82.3	74.9
	First	Whole	191.3	252.2	179.9	230.8	328.6	43.8	49.2	42.9	48.0	45.6
		LDK	223.7	370.5	223.2	353.7	523.8	64.1	81.9	78.7	92.2	84.1
Center	Top	Whole	165.7	226.1	203.4	203.7	257.6	48.9	56.6	52.5	52.1	50.7
		LDK	211.0	336.7	354.9	354.0	450.8	94.6	113.9	144.5	139.8	130.7
	Middle	Whole	198.5	204.0	183.6	185.8	257.7	37.3	37.9	38.0	38.1	36.2
		LDK	294.8	296.4	300.4	302.3	419.9	71.5	71.1	86.1	83.3	76.3
		MB	156.6	162.3	120.2	119.5	151.0	111.6	114.6	138.4	136.7	125.3
		C#1	265.1	290.3	194.5	203.9	257.6	128.3	135.7	156.3	160.5	156.1
	First	Whole	237.2	242.2	213.8	214.4	316.3	41.3	41.9	41.0	40.9	43.2
		LDK	359.1	359.3	353.9	353.1	523.2	78.7	78.3	92.7	89.3	82.0
West Corner	Top	Whole	188.7	236.0	187.4	225.5	292.5	60.7	66.2	56.1	61.1	60.7
		LDK	266.2	382.6	291.2	393.1	523.5	123.4	140.9	158.0	170.7	224.6
	Middle	Whole	162.9	220.6	159.6	208.3	278.8	39.7	45.6	38.8	44.1	42.6
		LDK	210.0	352.7	215.0	343.7	476.0	71.8	89.5	88.0	102.4	92.4
	First	Whole	194.4	252.4	187.3	237.3	338.3	43.4	49.1	42.1	47.2	45.8
		LDK	263.7	408.9	262.4	395.0	583.5	78.0	96.2	94.5	109.6	99.2
Detatched House		Whole	209.3	208.0	193.2	190.8	259.6	47.5	40.8	36.5	36.5	34.6
		LDK	377.2	371.6	365.6	361.6	512.5	88.0	88.3	104.5	100.6	91.0

Table 4 Summarized result of various dwelling types for cooling.

Cooling			Annual aggregated load [MJ/m^2]					TAC 2.5% maximum load [W/m^2]				
			Stochastic	Deterministic heat	Deterministic HVAC	Complete de-terministic #1	Complete de-terministic #2	Stochastic	Deterministic heat	Deterministic HVAC	Complete de-terministic #1	Complete de-terministic #2
East Corner	Top	Whole	190.0	173.4	239.0	223.9	274.1	69.4	68.6	64.7	63.2	62.3
		LDK	396.1	356.9	456.6	416.3	504.6	181.5	176.6	170.8	166.5	166.0
	Middle	Whole	31.8	22.6	49.3	38.9	47.5	21.7	19.8	21.2	19.9	18.3
		LDK	67.9	45.1	88.6	61.1	71.1	58.2	52.5	40.9	35.8	33.4
	First	Whole	13.4	8.6	25.3	18.9	22.0	16.1	13.6	15.1	13.7	12.7
		LDK	27.9	15.2	43.1	25.6	25.4	46.5	39.8	30.4	25.2	24.0
Center	Top	Whole	207.4	184.7	225.7	225.6	297.8	70.9	69.5	63.7	63.6	64.0
		LDK	402.6	355.4	419.7	420.5	548.6	182.0	176.7	167.0	167.8	169.4
	Middle	Whole	26.8	25.5	39.0	38.3	54.6	20.4	19.9	18.2	17.9	17.4
		LDK	46.3	45.1	62.7	61.9	76.9	51.8	51.9	36.1	36.8	35.9
		MB	6.3	5.3	19.7	20.2	26.0	64.8	61.9	49.8	51.1	47.0
		C#1	20.2	15.5	38.5	34.4	44.6	88.8	82.6	81.7	77.1	75.3
	First	Whole	10.3	9.9	18.6	18.3	31.3	14.3	13.8	12.4	12.3	12.4
		LDK	14.1	13.9	24.2	24.3	29.1	38.9	39.2	24.2	24.8	25.1
West Corner	Top	Whole	187.1	170.5	236.9	222.6	270.6	69.7	68.6	64.5	63.1	61.6
		LDK	411.3	369.9	472.9	433.1	520.7	192.2	186.6	179.1	174.7	173.5
	Middle	Whole	32.4	23.8	49.7	40.0	48.3	22.7	20.5	22.1	20.8	19.1
		LDK	73.2	50.9	93.2	66.5	75.8	64.5	58.5	45.2	39.7	37.0
	First	Whole	14.2	9.3	26.0	19.9	23.2	16.9	15.0	15.8	14.4	13.3
		LDK	30.9	17.8	46.3	28.7	28.2	51.5	45.0	33.0	27.4	25.5
Detatched House		Whole	47.2	46.6	79.8	81.1	111.9	36.7	30.9	32.8	33.2	34.2
		LDK	26.7	26.3	37.2	38.1	47.7	46.3	47.8	29.8	30.3	30.2

University of Science, was kind to give us the precious field measurement data. Committee members of "A study on pro-energy conservative living style in residential dwellings" in SHASE provided helpful suggestions to the study. We really appreciate the generous help extended.

REFERENCES

Akasaka, H. et al.; Expanded AMeDAS climate data, Architectural Institute of Japan (AIJ), 2000 (written in Japanese).

Mizutani, S., Inoue, T., Oguma, T.; Energy consumption for different uses in housing and energy usage, J. Environ. Eng. AIJ 609, 117-124, 2006 (written in Japanese with English abstract).

SHASE (Society of Heating, Air-conditioning and Sanitary Engineers of Japan) Technical Report; Inhabitants' behavior schedule and energy consumption in dwellings, 2000(written in Japanese).

Tanimoto, J., Hagishima, A., Sagara, H.; Validation of Probabilistic Methodology for Generating Actual Inhabitant's Behavior Schedules for Accurate Prediction of Maximum Energy Requirements, Energy and Buildings 43, 316-322, 2008 a.

Tanimoto, J., Hagishima, A., Sagara, H.; A methodology for peak energy requirement considering actual variation of occupants' behavior schedules, Building and Environment 43 (4), 610-619, 2008 b.

Tanimoto, J., Hagishima, A., Sagara, H.; Validation of Methodology for Utility Demand Prediction Considering Actual Variations in Inhabitant Behavior Schedules, Journal of Building Performance Simulation 1 (1), 1-12, 2008 c.

Tanimoto, J., Hagishima, A.; State transition probability for the Markov Model dealing with on/off cooling

schedule in dwellings, Energy and Buildings Vol. 37, pp. 181-187, 2005.
Tanimoto, J., Kimura, K.; Fundamental Study on the Indoor Humidity Regulation Characteristics of Porous Building Materials, International CIB W67 Symposium on Energy, Moisture and Climate in Building, I-37, 1990.

Appendix: Fundamental mathematical equations

Let us consider a heat balance equation at each nodal control volume after the space discrete operation.
The heat balance of node *i* at an exterior wall surface is,

$$0 = A_j C_{i,i-1}(T_i - T_{i-1}) + A_j h_{c\_out}(T_{out} - T_i) + A_j a_j \left((1 - AF_{balc,j})R_{s\_dir,j} + (f_{sky} - f_{balc,j})R_{s\_sky,j}\right) - A_j \varepsilon_j (f_{sky} - f_{balc,j})R_{noc}. \quad \cdots(1)$$

Subscript $i-1$ indicates adjacent to the surface node i, j means the facet containing node i, and *out* implies the outdoor air. A; faucet area [m^2], a; solar absorbance [ND], AF_{balc}; exterior wall area fraction avoided direct solar incidence by a sunshade [ND], C; heat conductance of the wall [$Wm^{-2}K^{-1}$], h_{c_out}; outside convective heat transfer coefficient [$Wm^{-2}K^{-1}$], f_{sky}; sky view factor [ND], f_{balc}; view factor from the faucet to sunshade [ND], ε; emissivity [ND], R_{noc}; nocturnal radiation rate [Wm^{-2}], R_{s_dir}, R_{s_sky}; direct and sky solar radiation rates [Wm^{-2}], T; temperature [K].
The heat balance of node *i* within a wall is,

$$A_j \Delta x_i CPG_i \frac{dT_i}{dt} = A_j C_{i,i-1}(T_i - T_{i-1}) + A_j C_{i,i+1}(T_{i+1} - T_i). \quad \cdots(2)$$

Subscript $i+1$ and $i-1$ mean the adjacent nodes of i, t; time [s], Δx; discrete length [m], CPG; specific heat [$Jm^{-3}K^{-1}$].
The heat balance of node *i* on an interior wall surface is,

$$0 = A_j C_{i,i-1}(T_{i-1} - T_i) + A_j h_{c\_in,j}(T_r - T_i) + C_b \sum_{k=1}^{N_f} A_k \varepsilon_k G_{k,j}(T_{surf,k} - T_i) + P_j. \quad \cdots(3)$$

T_r; room air temperature [K], $T_{sur,k}$; surface temperature if faucet k [K], h_{c_in}; interior convective heat transfer coefficient [$Wm^{-2}K^{-1}$], C_b; radiation constant for a black body (Stefan-Bolzmann Constant*10^8) [$Wm^{-2}K^{-4}$], N_f; total number of walls in the room [ND], $G_{k,j}$; Gebhart's factor (absorbed ratio at faucet j to emitted radiation rate from faucet k, including the multi-reflection effect from the inner walls), P_j; production term at faucet j [W]. P_j relates to the radiative factor of the indoor anthropogenic heat generation and transmitted solar radiation rate through windows. The former is distributed by weight of the respective area, the latter is entirely absorbed by the floor. Infrared radiation rate emitted from a wall surface can be linearized by assuming the surface temperature coefficient as 1.
Transmitted solar radiation rate through windows $R_{tra,j}$ can be,

$$R_{tra,j} = A_j \left(R_{s\_dir,j} \cdot \tau_{total\_dir,j} + R_{s\_sky,j} \cdot \tau_{total\_sky,j}\right), \quad \cdots(4)$$

here, $\tau_{total\_dir,j}$; overall transmittance of opening faucet j (consisting of a glazing window and a curtain) for direct solar radiation considering multi-reflection [ND], $\tau_{total\_sky,j}$; similar for sky solar radiation [ND]. Dependencies on solar incidental angle for glazing transmittance and absorbance are fully considered.
The heat balance of node for room air is,

$$V_r(CPG_{air} + CPG_{fur})\frac{dT_r}{dt} = \sum_{k=1}^{N_f} A_k h_{c\_in,k}(T_{surf,k} - T_r) + n_r V_r CPG_{air}(T_{out} - T_r) + P_r - H_{S\_ext}, \quad \cdots(5)$$

where, CPG_{air}; specific heat of humid air [$Jm^{-3}K^{-1}$], CPG_{fur}; equivalent specific capacity of furniture per unit room air volume [$Jm^{-3}K^{-1}$], n_r; air change rate [s^{-1}], V_r; air volume of room r [m^3], P_r ; production term at room r [W] (derived from indoor anthropogenic heat generation consisting of the convective elements of electric household appliances and human sensitive heat exhaustion), H_{S_ext}; sensitive heat extraction rate from the room (indicating the cooling/heating load if positive/negative) [W]. In the thermal load calculation mode, T_r should be assumed to be set at room air temperature T_{set} [K] (not only for Equation (5), but for all heat balance equations containing the room air node), and H_{S_ext} must be one of the unknown variables. In the room air temperature calculation mode, T_r must be one of the unknown variables while $H_{S\_ext} = 0$.
The water vapor balance for room air is,

$$V_r \gamma_{air} \frac{dX_r}{dt} = n_r V_r \gamma_{air}(X_{out} - X_r) + PX_r - H_{L\_ext}/l, \quad \cdots(6)$$

where, γ_{air}; specific weight of humid air [gm^{-3}], X_{out}, X_r; absolute humidity of outdoor air and room air [g/g'], P_r; water vapor production at room r [g/s] (relating to the human latent heat generation and other vapor sources, such as cooking), l; latent heat of water [J/g], H_{L_ext}; latent heat extraction rate from the room (positive indicates dehumidifying and negative indicates humidifying load) [W]. In the thermal load calculation mode, $X_r = X_{set}$ (set air humidity [g/g']) and H_{L_ext} must be an unknown variable. Whereas, in the room humidity calculation mode, X_r must be one of the unknown variables while $H_{L\_ext} = 0$.
Aggregating all sensitive heat transfer equations (Eq. (1) – (5)), in the dwelling, a single vector-matrix equation can be drawn. Namely,

$$\mathbf{M}\frac{d\{x\}}{dt} = \mathbf{C}\{x\} + \mathbf{C_o}\{x_o\} + \{P\}, \quad \cdots(7)$$

where, $\mathbf{M}$; heat capacitance matrix, $\mathbf{C}$; heat conductance matrix, $\mathbf{C_o}$; heat capacitance matrix connecting with given temperature boundaries by heat transfer of either convection or air change, $\{x\}$; unknown variables vector, $\{x_o\}$; vector for given temperature boundaries, $\{P\}$; vector for production terms.
Equation (7) can be rewritten after time discrete operation,

$$\{x\}_{m+1} = [\mathbf{M} - r\mathbf{C}]^{-1}\{[\mathbf{M} + (1-r)\mathbf{C}]\{x\}_m + \mathbf{C_o}\{(1-r)\{x_o\}_m + r\{x_o\}_{m+1}\} + \{(1-r)\{P\}_m + r\{P\}_{m+1}\}\}, \quad \cdots(8)$$

where, subscript m indicates time step. r implies time discrete parameter (the scheme is time-forward finite difference method, time-backward finite difference method or Crank-Nicolson finite difference method, if $r = 0$, 1 or 0.5).
Combining Equation (8) with time discrete (6) simultaneously, we can conduct a sequence of time step calculation, which leads to solving of unknown variables such as respective nodal temperatures, humidity, and thermal load of the room without any iterative procedure (because all equations have been expressed by linear forms). There are 159 unknown variables in the case of an east center dwelling in the middle floor of the apartment.